Heterogeneous & Homogeneous & Bio- & Nano-
CHEMCATCHEM
CATALYSIS

Accepted Article

Title: Surface--passivated hierarchically structured ZSM--5 zeolites: highperformance shape-selective catalysts for para-xylene production

Authors: Jian Lv, Zile Hua, Jian Zhou, Zhicheng Liu, Hangle Guo, and Jianlin Shi

To be cited as: *ChemCatChem* 10.1002/cctc.201800044

Link to VoR: http://dx.doi.org/10.1002/cctc.201800044

A Journal of
ChemPubSoc Europe

WILEY-VCH

www.chemcatchem.org

10.1002/cctc.201800044

WILEY-VCH

FULL PAPER

Surface-passivated hierarchically structured ZSM-5 zeolites: high-performance shape-selective catalysts for *para*-xylene production

Jian Lv,[a,b] Zile Hua,*[a] Jian Zhou,[c] Zhicheng Liu[c], Hangle Guo[a,b] and Jianlin Shi*[a]

Abstract: Hierarchically structured ZSM-5 zeolites (HSZ) were synthesized and used as high-performance catalysts for *para*-xylene (*p*-X) production by tuning their pore structures and external surface acidity, which was achieved by two independent passivation approaches: dealumination in oxalic acid solution and chemical liquid deposition of tetra-ethoxysilane (CLD of TEOS). Various materials characterization techniques showed that the mesoporous structures of HSZ were well preserved after dealumination or CLD of TEOS, and more importantly, the external surfaces of HSZ were passivated significantly. Compared to dealumination, CLD seems to be more efficient because not only the external surface could be passivated, but also the pore-openings of HSZ had been effectively narrowed, which both favored the enhancement of product *p*-X selectivity in *ortho*-xylene (*o*-X) isomerization. Constraint index (CI) of as-synthesized catalysts derived from the competitive reactions of ethylbenzene (EB) dealkylation and *meta*-xylene (*m*-X) isomerization and gravimetric adsorption measurements were introduced to investigate the extent of pore-narrowing by CLD of TEOS. Benefitting from the auxiliary mesopores and surface-passivation treatments, the optimized catalyst HSZ(Si0.5) showed remarkably enhanced catalytic activity of ~42% and *p*-X selectivity of ~50%, simultaneously, in sharp comparison to ~13% and ~45%, respectively, over the microporous ZSM-5 counterpart in the model reaction of *o*-X isomerization.

Introduction

Para-Xylene (*p*-X) is a valuable aromatic compounds used as the raw materials for the productions of terephthalate and polyester [1]. In petrochemical industries, the aromatics, such as xylene, are usually produced by catalytic reforming and naphtha pyrolysis. In these process, thermodynamic equilibrium mixtures of xylene isomers (*o*-/*m*-/*p*-) along with other aromatics are produced, which means that the value-added target product *p*-X will be obtained at the high cost of other less valuable isomers' over-production. Because these three isomers have similar boiling points and molecular size, the product purification is rather difficult and energy intensive [2]. Thus, selective production of *p*-X through disproportionation, alkylation and isomerization are of great significance and gaining more and more attentions [1b, 2b, 3]. To increase selectivity towards *para*-isomer, catalysts with excellent shape-selectivity are indispensable. In this respect, ZSM-5 zeolites are well known and promising candidates because of its 10-membered ring (MR) pore system with MFI topography, the size of which is comparable to *p*-X molecules [4]. On the other hand, the sole presence of microporous structure in purely ZSM-5 zeolites often leads to mass transfer limitation and the internal acid sites of ZSM-5 cannot be utilized adequately. As a result, its catalytic activity in bulky aromatic transformations is far from being satisfactory. Besides, the micropores of ZSM-5 will easily be blocked by coking, which could cause rapid catalyst deactivation [5]. New catalysts with well-engineered pore structure and dimension and excellent activity and high *p*-X selectivity are highly desired.

It has been reported that introducing additional mesoporous structures in microporous zeolites, which is known as hierarchically structured zeolites (HSZ), will lead to much facilitated mass transfer therein and enhanced anti-deactivation ability [5, 6]. But in the meantime the newly introduced mesoporous structure brings more external surface acid sites to the catalyst. The external surface acid sites lack shape-selective control as compared to acid sites located in the internal microporous structure of ZSM-5 zeolites [7c], which is responsible for the undesired side reactions and decrease the product *p*-X selectivity [3, 7]. So HSZ always show poorer *para*-selectivity as compared to microporous zeolites in spite of their higher catalytic activity [8]. The above characters make HSZ not suitable for functioning as shape-selective catalysts. Thus, to enhance the *para*-selectivity of HSZ while keeping its mesostructure and high catalytic activity, one of the best way is to selectively passivate or de-activate its external surface acid sites.

According to previous reports, the passivation of external surface of ZSM-5 zeolites has been adopted by various post-treatments, such as impregnating with B, Mg and P elements [2b, 9], coating of inert silicalite-1 layers [10a], chemical liquid deposition (CLD) of tetra-ethoxysilane (TEOS) [2b, 3, 7a, 11] and mechanochemical approaches [7b]. However, in most cases, these passivation treatments always lead to the decrease of zeolite catalyst activity because of the pore blockage and/or loss of acid sites. For example, Li et al. modified ZSM-5 zeolites with P element and found that, in the reaction of toluene disproportionation, the conversion of toluene decreased from 56.3% to 22.6% with the increase of P amount from 0.94 wt% to 4.86 wt%, while the product *p*-X selectivity increased from 23.4% to 84.1% [9c]. By CLD of TEOS, the resultant ZSM-5 materials

[a] Dr. J. Lv, Prof. Dr. Z. Hua, MS. H. Guo and Prof. Dr. J. Shi.
State Key Laboratory of High Performance Ceramics and Superfine Microstructure
Shanghai Institute of Ceramics, Chinese Academy of Sciences 1295 Dingxi Road, Shanghai 200050, PR China
E-mail: jlshi@mail.sic.ac.cn; huazl@mail.sic.ac.cn
[b] Dr. J. Lv and MS. H. Guo
University of Chinese Academy of Sciences
19 Yuquan Road, Beijing 100049, P. R. China.
[c] Dr. J. Zhou, Dr Z. Liu
Sinopec Shanghai Research Institute of Petrochemical Technology
1658 Pudong North Road, Shanghai 201208, P. R. China.

Supporting information for this article is given via a link at the end of the document

showed the decreased acid amount. Accordingly, in the followed reaction of ethylbenzene (EB) disproportionation, the conversion of EB decreased by ~10% [10b]. Therefore, it holds much promise if we can combine the superior catalytic activity of HSZ and high *para*-selectivity of surface-passivated zeolites in the reaction of *o*-X isomerization.

Here in this study, a strategy of passivating the external surface of as-synthesized HSZ for enhanced activity and high selectivity towards *p*-X production is reported. Firstly, HSZ was synthesized by a mesoporogen-free synthetic route previously reported by our group [12a]. Then the external surface acidity of HSZ was fine-tuned by dealumination in oxalic acid solution or CLD of TEOS. Compared to the typical micropore size (~0.55 nm) of ZSM-5 zeolite, TEOS molecules (1.03nm) and trioxalato aluminium complexes (0.64nm) [12b] are too large to freely diffuse in the micropore systems and as a result, the external surface of HSZ could be selectively passivated. The obtained samples were characterized by TEM, SEM, N_2 absorption/desorption, NH_3-TPD and catalytic cracking of 1,3,5-triisopropylbenzene (TIPB) to illustrate the changes of its external acidity and pore structures after passivation. In addition, constraint index (CI) about the competitive reaction of EB dealkylation and *meta*-xylene (*m*-X) isomerization was introduced to evaluate the extent of pore narrowing caused by dealumination or CLD of TEOS. The impact of surface passivation treatments on catalysts' activity and *para*-selectivity were investigated in the model reaction of *ortho*-xylene (*o*-X) isomerization.

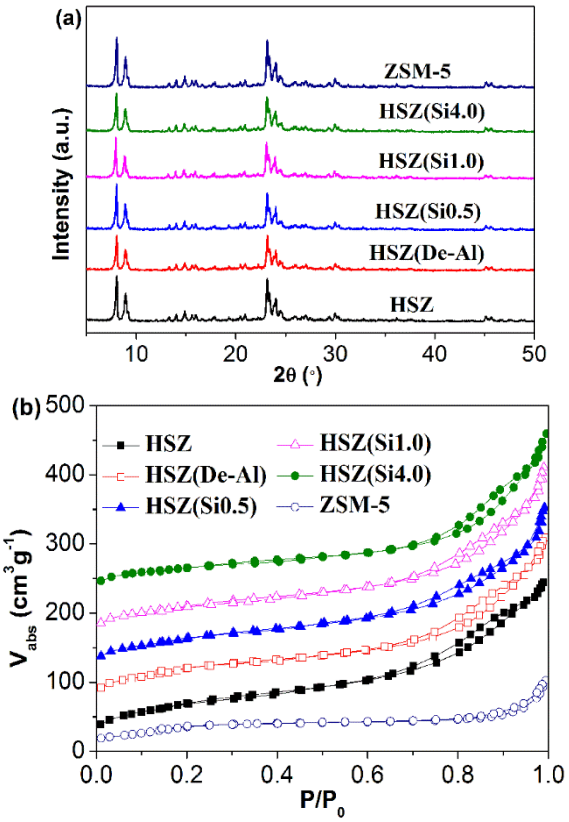

Fig.1 (a) XRD patterns and (b) N_2 adsorption/desorption isotherms of all as-synthesized materials.

Results and Discussion

Fig. 1a is the XRD patterns of synthesized HSZ series materials and microporous ZSM-5 zeolites in the 2 theta range of 5 ~ 50°. All of them demonstrate the typical and similar diffraction patterns of MFI-type zeolite irrespective of post-synthesis dealumination or CLD of TEOS treatment, indicating their high crystallinity and high stability [2a, 5, 12a]. Fig. 1b shows their N_2 sorption isotherms and the textural properties are summarized in Table 1. Among them, sample ZSM-5 exhibits the typical type-I profile of microporous materials due to the absence of mesoporosity. Its corresponding apparent surface areas (S_{BET}), external surface area (S_{ext}) and total pore volume (V_{total}) are 370 m^2g^{-1}, 160 m^2g^{-1} and 0.22 cm^3g^{-1}, respectively. In contrast, the isotherms of HSZ series materials are the type-IV profile with a hysteresis loop and an apparent uptake at elevated relative pressures, indicating the presence of abundant mesoporous structures. The most probable apertures of HSZ series are about 17 nm. Although the N_2 sorption isotherms and pore size distribution curves (Fig. S1) of surface-passivated HSZ materials keep the original characteristics of parent HSZ, the lower S_{BET} and S_{ext} values are obtained in comparison with those of parent HSZ. In this regard, the decrease with SiO_2-deposited HSZ is more significant resulting from the partial blockage of micro-/mesoporous channels, whereas the impact on sample HSZ(De-Al) is insignificant. Specifically, the S_{BET}, S_{ext} and V_{total} values of

Table 1. The physicochemical properties of as-synthesized materials.

Entry	Samples	S_{BET} (m^2g^{-1})	S_{ext} (m^2g^{-1})	V_{total} (cm^3g^{-1})	V_{meso} (cm^3g^{-1})	V_{micro} (cm^3g^{-1})	Si/Al	Acid sites (mmol/g)	
								Weak acid	Strong acid
1	HSZ	411	272	0.42	0.35	0.07	47	0.316	0.137
2	HSZ(De-Al)	386	257	0.41	0.34	0.07	80	0.183	0.114
3	HSZ(Si0.5)	343	217	0.39	0.33	0.06	47	0.303	0.129
4	HSZ(Si1.0)	341	212	0.38	0.32	0.06	48	0.297	0.124
5	HSZ(Si4.0)	301	161	0.37	0.30	0.06	49	0.273	0.083
6	ZSM-5	370	160	0.22	0.12	0.10	44	0.279	0.156

HSZ(De-Al) and HSZ(Si0.5) are 386 and 343 m^2g^{-1}, 257 and 217 m^2g^{-1}, 0.41 and 0.39 cm^3g^{-1}, respectively. On the other hand, Fig. 2a-b and Fig. S3 are the SEM images of all materials. Apparently, regardless of dealumination or CLD treatment, the materials morphology remains unchanged. As shown in Fig. 2a-b and Fig. S3, all materials consist of spherical particles of ~1 μm in diameter in which abundant mesopores of 15-20 nm in size can be found under their rough surfaces consistent with above N_2 sorption results. In TEM images of Fig. 2c &2d, the oriented lattice fringes on the edge of particles and the discrete and bright SAED patterns confirm the single-crystalline nature of synthesized HSZ series. In contrast, microporous ZSM-5 shows typical coffin shape with smooth surfaces (Fig. S3d).

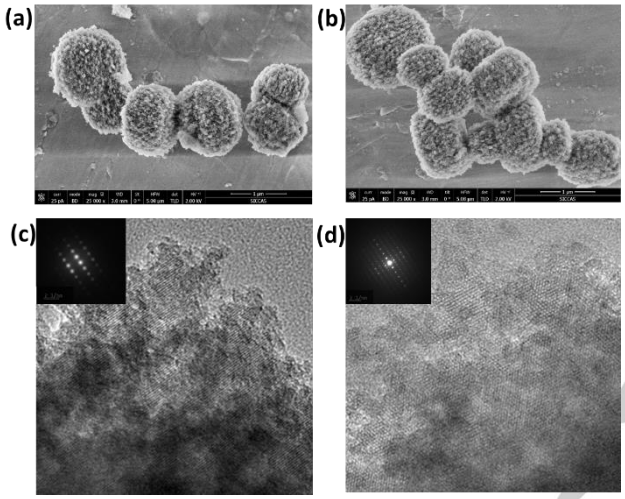

Fig 2. SEM images of (a) HSZ(Si0.5) and (b) HSZ(De-Al); High-resolution TEM image and selected area electron diffraction pattern (inset) of (c) HSZ(Si0.5) and (d) HSZ(De-Al).

Table 1 lists the Si/Al ratios of synthesized HSZ series and microporous ZSM-5. Resulting from the successful acid dealumination, sample HSZ(De-Al) possesses the highest Si/Al ratio of 80, while the other materials keep the ratios between 47 and 49. Accordingly, Fig. 3a gives the NH_3-TPD profiles of HSZ series and microporous ZSM-5 and the calculated acid amounts are listed in Table 1. All of HSZ series feature two desorption bands similar to that of microporous ZSM-5, in which the high temperature and low temperature band correspond to the strong and the weak acid sites respectively [9b, 9c, 12a]. Because the strong acidity of ZSM-5 zeolites originates from the isomorphous substitution of framework Si by Al, the change of Al content and/or Al coordination state would induce the variation of acid amount and/or acid strength. For parent HSZ, the broadened high-temperature bands reflect the presence of a large amount of strong acid sites of relatively weaker acid strength resulting from the disordered framework Al sites on the external surface of HSZ. Previous reports also reported similar results, indicating that the acid sites on external surface show different acidity from those inside the microporous structures [18]. Accompanied by the increase of SiO_2-deposition amount, the gradual decrease of high-temperature signal intensity and strong acid amount confirms the successful passivation of external acid sites on HSZ. On the other hand, for sample HSZ(De-Al), since about 40% of Al species has been extracted (Table. 1), the decreases of high-temperature band intensity and strong acid amount appear more significant. Interestingly, because of the oxalic acid dealumination, the broadened high-temperature desorption band of parent HSZ become sharpened and the resultant profile of HSZ(De-Al) gets similar to that of microporous ZSM-5, which confirms the diminishing of medium strength acid sites and achievement of selective dealumination on the HSZ external surfaces. In addition, ^{27}Al MAS NMR analyses have also been conducted to investigate the chemical states of Al species of synthesized HSZ series and microporous ZSM-5. Similar to the typical ^{27}Al MAS NMR profile of microporous ZSM-5 (Fig. 3b), a major peak can be observed at ~53 ppm for HSZ series, assigned to the tetrahedrally coordinated framework Al with strong Brønsted acidity [13], which means that the chemical state of Al atoms is not obviously changed by the surface-passivation treatments.

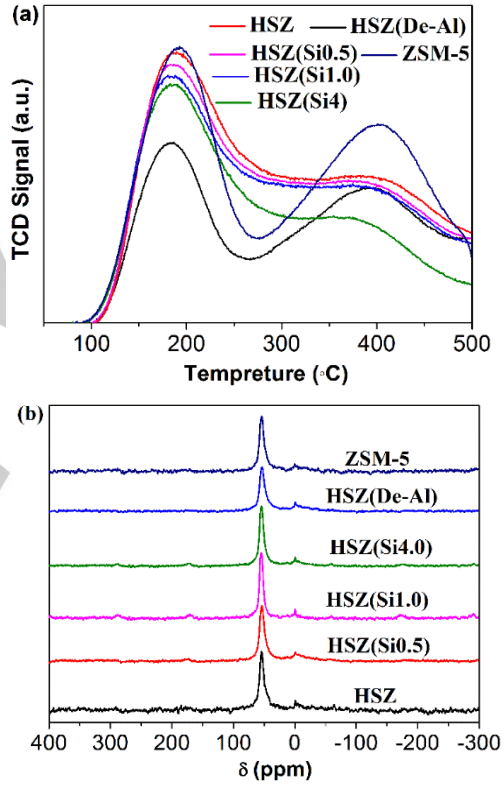

Fig 3. (a) NH_3-TPD profiles and (b) ^{27}Al MAS NMR spectra of as-synthesized materials.

Further, to demonstrate the variation of surface acidity of HSZ materials before and after surface modification, a model reaction of TIPB cracking has been carried out. The kinetic diameter of TIPB molecule is about 0.95 nm, which is larger than the micropore size of ZSM-5 zeolites of 0.55 nm. Therefore, the TIPB cracking can only occur at the external surface of catalyst particles or at the micropore mouths [7b, 14]. As a result, microporous ZSM-5 only offers the initial TIPB conversion of ~70%, as shown in Table 2. In contrast, parent HSZ exhibit a higher initial conversion of 90% due to its abundant mesoporous structures. Because of the selective dealumination of the external surface area, the initial conversion with sample HSZ(De-Al) decreases to 45% which is even much lower than that of

microporous ZSM-5 counterparts. Comparatively, the initial conversion of TIPB by SiO_2-deposited HSZ gradually decreases from 90% to 76%, 64% and 24% as the amount of deposited SiO_2 is increased from 0.5 wt% to 1 wt% and 4 wt%, indicating that the successful external surface passivation of HSZ by CLD of TEOS. The above results demonstrate that all post-synthesis treatments adopted in this research have achieved selective passivation on the external surface of HSZ as expected.

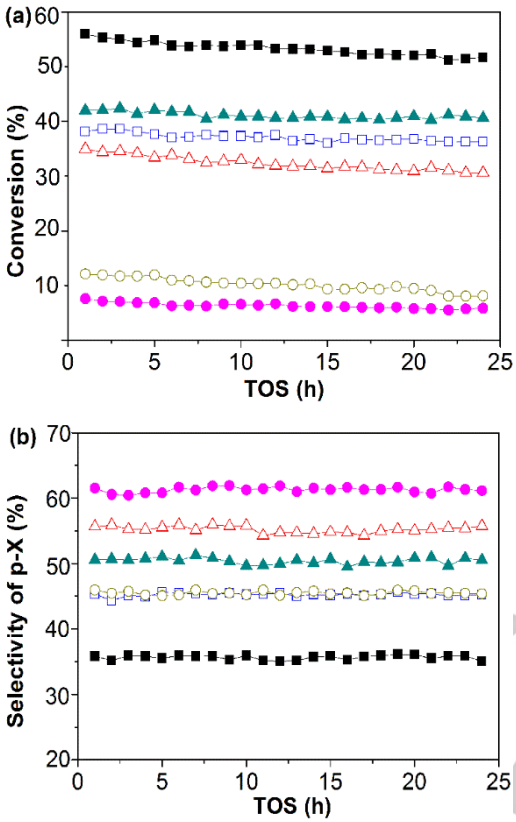

Fig 4. (a) Conversion of *o*-X (b) Selectivity of *p*-X over as-synthesized materials in the model reaction of *o*-X isomerization (HSZ ■, HSZ(De-Al) □ , HSZ(Si0.5) ▲, HSZ(Si1.0) △, HSZ(Si4.0) ●, ZSM-5 ○).

Fig. 4 shows the catalytic performance of HSZ series and microporous ZSM-5 in the isomerization of *o*-X to *p*-X. In general, besides the xylene isomers (*o*-/*m*-/*p*-X), there is no other hydrocarbons detected in the effluent. And during the testing period of 24 h, the deactivation of all catalysts is insignificant. As previously reported [8a], benefitting from the auxiliary mesoporous structures, parent HSZ exhibits an initial conversion of *o*-X as high as 56%, which is four times that of microporous ZSM-5 counterparts (~13%). However, suffering from its larger external surface area and consequently more external acid centers, the product selectivity of *p*-X with parent HSZ is as low as ~35%, which is significantly lower than 46% over ZSM-5. This means that the undesired external surface acid sites of HSZ which lacks shape-selective control promote side reactions, leading to the lowered product *p*-X selectivity. Fortunately, when HSZ(De-Al) or SiO_2-passivated HSZ materials (except sample HSZ(Si4.0)) were used, superior catalytic performances, not only the high activity but also the enhanced or comparable *p*-X selectivity, were achieved. Specifically, the conversion of *o*-X over sample HSZ(De-Al) is ~39%, which is three times that of microporous ZSM-5, while both of them shows the approximately the same *p*-X selectivity of ~45%. Considering the variation of materials textural properties before and after dealumination treatment is insignificant, as shown in Fig. 1a and Table 1, the enhanced *para*-selectivity for HSZ(De-Al) could be mainly attributed to the selective passivation of external surface active centers which suppresses the possible non-selective isomer interconversion, in consistence with the above NH_3-TPD and TIPB cracking results (Fig. 3a and Table 2). In comparison, the effect of SiO_2 deposition on HSZ on the *o*-X to *p*-X isomerization is more pronounced than dealumination. As shown in Fig. 4b, the increase of SiO_2-deposition amount from 0.5 wt% to 4.0 wt% leads to the marked increase of *p*-X selectivity from ~35% to ~62%, while the *o*-X conversion decreases from ~56% to ~8%. Although the positive effect of selective passivation on the external surface acid sites is dominant as happened on sample HSZ(De-Al), the other critical factor, i.e., pore-narrowing effect, should be considered in enhancing the *p*-X selectivity over SiO_2-passivated HSZ as compared to that of microporous ZSM-5 because SiO_2 deposition could partially block the pore-openings and enlarge the diffusivity difference of xylene isomers [15a-b].

In order to characterize the pore size variation and/or Al distribution in zeolite catalysts, Constraint Index (CI) has been designed basing on the competitive reactions of two reactants with differentiated molecular size [15]. Among them, Bhat et al had ever studied the pore size reduction of zeolites caused by silica deposition through the competitive reaction between EB dealkylation and *m*-X isomerization and the CI was defined as $Log(1-X_{EB})/Log(1-X_{m\text{-}X})$ in which X_{EB} and $X_{m\text{-}X}$ represent the conversions of EB and *m*-X, respectively [15a]. Higher CI means more significant pore-narrowing. Herein, the competitive reaction between EB dealkylation and *m*-X isomerization was adopted to clarify the pore-narrowing effect and the subtle variation of pore-openings of surface-passivated HSZ. As shown in Table 2, the conversions of EB and *m*-X over microporous ZSM-5 are 25% and 16%, respectively, and the calculated CI is 1.65, which is close to previous results reported by Bhat et al [15a]. For parent HSZ, due to the introduction of additional mesoporous structures and consequently the decreased diffusion limitation of the relative bulky *m*-X molecules, higher conversion of *m*-X of 30% has been obtained as expected, while the conversion of EB decreased to 16% resulting from the competitive adsorption of *m*-X molecules and the much higher activation energy of EB dealkylation (~186 KJ/mol) as compared to that of *m*-X isomerization (47~54 KJ/mol) [16]. Consequently, the corresponding CI of HSZ decreases to 0.49. In comparison, because of the reduction of active acid site amounts by the dealumination treatment, the *m*-X and EB conversions over sample HSZ(De-Al) consistently decrease to 25% and 13%, respectively. But interestingly, the calculated CI is 0.48, almost the same as that of parent HSZ, which reflects the maintenance of pore structures of HSZ through the post-synthesis dealumination treatment. In addition, although the conversion of *m*-X over SiO_2-deposited HSZ series decrease gradually from 30% of parent HSZ to 7% with the increase of SiO_2-deposition amount up to 4.0 wt%, the variation of EB conversion is non-unidirectional, which first decreases to 13%, then increases to

25% and finally decreases again to 23%, demonstrating the complicated effects of SiO_2-passivation on the materials acidity and textural properties. Specifically, for the relative bulky *m*-X molecules, both the decrease of surface acid site amounts and the pore narrowing effect by SiO_2 deposition contribute to the decrease of *m*-X conversion. However, in the EB conversion, although the decrease of external active acid site amounts in SiO_2-passivated HSZ would result in lowered catalyst activity, its small molecule size allows EB molecules to diffuse much more freely in the micropore channels than bulky *m*-X molecules, and consequently resulting in its higher concentration in micropore channels in comparison with *m*-X molecules, especially in the pore-narrowed HSZ series. In addition, the amorphous deposited SiO_2 coating on zeolite surfaces might enhance the adsorption possibility of organic reagents from gas phase to the catalyst surface and then into the micropores, which may also favor the diffusion of EB molecules within the micropore channels due to its relative small size [17a, b]. As a result, when HSZ(Si0.5) was used, the EB conversion decreased slightly from 16% to 13% (by ~18%), whereas the conversion of *m*-X decreased much more significantly from 30% to 18% (by ~40%). Moreover, although the *m*-X conversion over HSZ(Si1.0) catalyst with higher amount of SiO_2 passivation continues to decrease to 14%, the EB conversion in contrast increases to 25% over the same catalyst. Correspondingly, the calculated CI are 0.70, 1.90 and 3.60 (Fig. S4), respectively, for sample HSZ(Si0.5), HSZ(Si1.0) and HSZ(Si4.0), which confirms the continuous pore-narrowing effect by SiO_2-deposition in HSZ.

Table. 2 Results of TIPB cracking and competitive reactions between EB and *m*-X over as-synthesized materials and ZSM-5.

Samples	TIPB Conversion (%)	EB and *m*-X competition reaction		
		EB Conversion (%)	*m*-X Conversion (%)	CI
HSZ	90	16	30	0.49
HSZ(De-Al)	45	13	25	0.48
HSZ(Si0.5)	76	13	18	0.70
HSZ(Si1.0)	64	25	14	1.90
HSZ(Si4.0)	24	23	7	3.60
ZSM-5	70	25	16	1.65

To further verify the pore-narrowing effect caused by post-synthesis dealumination and CLD of TEOS treatment, gravimetric adsorption measurements was conducted using *m*-X and EB as probe molecules. The normalized amount of *m*-X and EB uptake was shown in Fig. 5. It can be observed that there was a good linear relationship between the normalized uptake amount (M_t/M_∞) and $t^{1/2}$, which is consistent with previous reports [17a, c]. The diffusion time constants (D/r^2) can be derived from slopes ($6\cdot\pi^{-1/2}\cdot(D/r^2)^{1/2}$) of fitting lines, as shown in Fig. 5 and Table. 3. For bulky *m*-X molecules, parent HSZ and sample De-Al got the approximate diffusion time constants of 7.04×10^{-5} s^{-1} and 7.24×10^{-5} s^{-1}, indicating that dealumination does not lead to the significant change on HSZ pore structures, which is consistent

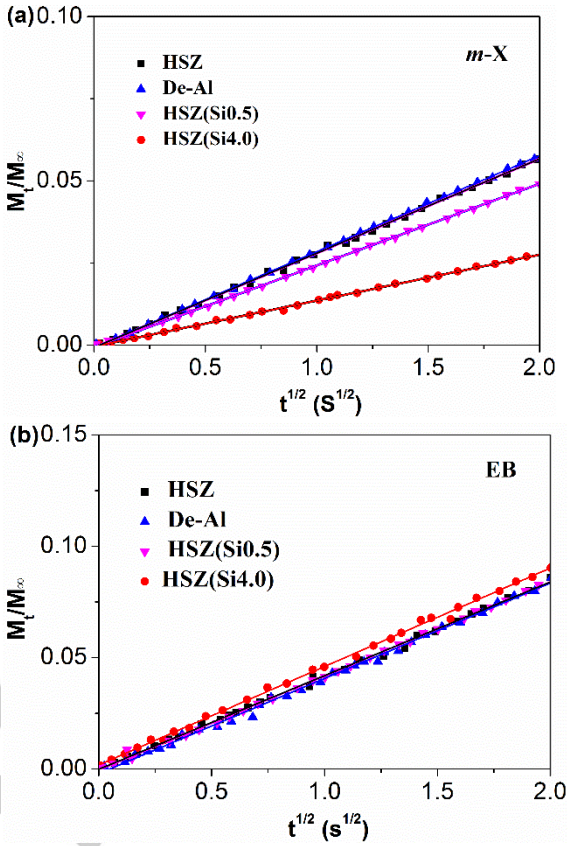

Fig 5. Normalized amount of adsorption profiles of (a) *m*-X and (b) EB over HSZ and passivated samples under 0.5 mbar at 25 ℃ in a short time domain.

with above N_2 sorption and CI results. However, for SiO_2-deposited HSZ(Si0.5) and HSZ(Si4.0), the diffusion time constants decreased from 7.04×10^{-5} s^{-1} to 5.24×10^{-5} s^{-1} and 1.66×10^{-5} s^{-1}, respectively, which strongly suggest that the diffusion of *m*-X in modified HSZ is significantly retarded resulting from the CLD-of-TEOS-induced pore-narrowing. On the other hand, when the EB molecules with smaller kinetic diameter as compared to *m*-X were adopted as sorbates, the diffusion time constants of EB in HSZ was 1.54×10^{-4} s^{-1}, significantly higher than the diffusion time constants of *m*-X. After CLD of TEOS, the diffusion time constants of EB in HSZ(0.5) (1.56×10^{-4} s^{-1}) and HSZ(4.0) (1.70×10^{-4} s^{-1}) were nearly unchanged as compared to HSZ (1.54×10^{-4} s^{-1}), which means although the pore-openings of HSZ were narrowed by CLD, EB molecule still can diffuse into the micropores easily due to its small molecule size. Accordingly, the conversion of EB in the above competitive reactions would decrease at a slower rate or even was promoted after CLD of TEOS because the diffusion of *m*-X was retarded by pore-narrowing while the diffusion of EB molecules were nearly unaffected. Indeed, we can observe that the EB conversion decreased slightly from 16% of HSZ to 13% of HSZ(Si0.5), and then increased to 25% of HSZ(1.0). Similarly, in *o*-X isomerization, the pore-narrowing of HSZ enlarges the diffusivity differences among xylene isomers, which selectively retains bulkier *o*-X and *m*-X molecules in the micropores, facilitates their further

transformation to *p*-X and results in the enhanced *para*-selectivity in the products.

Table. 3 Diffusion time constants of *m*-X and EB in parent and surface passivated HSZ.

Diffusion time constant (s^{-1})	Samples			
	HSZ	De-Al	HSZ(Si0.5)	HSZ(Si4.0)
***m*-X**	7.04×10^{-5}	7.24×10^{-5}	5.24×10^{-5}	1.66×10^{-5}
EB	1.54×10^{-4}	1.60×10^{-4}	1.56×10^{-4}	1.70×10^{-4}

Conclusions

In summary, by tailoring the external surface acidity and pore structures of HSZ *via* dealumination in oxalic acid solution or CLD of TEOS, we synthesized surface-passivated HSZ which performs well in the reaction of *o*-X isomerization. As compared to dealumination, CLD approach seems to be more efficient in enhancing the shape-selectivity of HSZ because not only the external surface of HSZ has been passivated, but also its pore-openings have been effectively narrowed as demonstrated by EB and *m*-X competitive reactions and gravimetric adsorption measurements, both of which are beneficial to enhancing the *p*-X selectivity in the model reaction of *o*-X to *p*-X isomerization. Over the optimally tailored HSZ sample, HSZ(Si0.5), both the relatively high catalytic activity (~42% conversion) and enhanced shape-selectivity (~50% *p*-X selectivity) have been simultaneously achieved, which are remarkably higher than the conversion (~13%) and *p*-X selectivity (~45%) of microporous ZSM-5 counterparts.

Experimental Section

Chemicals

Tetra-ethoxysilane (TEOS, AR grade) was purchased from Shanghai Lingfeng Chemical Co. Aluminum isopropoxide ($Al(iPrO)_3$, AR grade) was purchased from Adamas reagent Co. Ltd. Tetrapropylammonium hydroxide (TPAOH, 25 wt% in water) was obtained from Yixing Dahua Chemical Co. Ammonia chloride (NH_4Cl, AR grade), n-hexane (AR grade) and oxalic acid (AR grade) were purchased from Sinopharm Chemical Reagent Co. *O*-xylene, *p*-xylene, *m*-xylene, 1,3,5-triisopropylbenzene and diethylbenzene was got from Sigma-Aldrich reagent Co. ZSM-5 zeolites (Si/Al = 50) were purchased from Nankai University Catalyst Factory. All reagents were used directly without any purification.

Materials preparation

Synthesis of HSZ: According to the previously reported procedures [12a], 10.41 g TEOS, 0.2042 g $Al(iPrO)_3$ and 18.0 g H_2O was mixed under room temperature for 0.5 h at first. Then, 4.1 g TPAOH (25 wt% aqueous solution) was added dropwise and then aged at 40 ℃ for 48 h. Subsequently, the resultant gel was crushed and transferred into three crucibles. We put each crucible into a Teflon-lined stainless autoclave. Subsequently, 0.7 g deionized water was added into the bottom of Teflon liner, but outside the crucible container. The autoclave was heated in an oven at 150 ℃ for 10 hours. The final product was washed by deionized water for 3 times and dried in an oven at 80 ℃ overnight. Then, the organic structure-directing-agents was removed by calcination at 550 ℃ for 6 h.

Ion exchange of HSZ: 1.0 g synthesized HSZ was added into 100 ml NH_4Cl solution (1 M). and stirred at 80 ℃ for 4h. This procedure was repeated 3 times. Then, ion-exchanged samples were dried and calcined at 550 ℃ for 4 h to make the catalysts to be H-type.

Dealumination of HSZ: 1.0 g HSZ (H-type) and 20 ml oxalic acid solution (2M) were add into three-necked flask. It was stirred at 500 rpm under reflux for 10 h. Then the sample was filtered and washed by deionized water. The as-collected powder was dried at 120 ℃ for 6 h. The above procedure was repeated for 3 times. At last, the sample was calcined at 550 ℃ for 4 h. The as-synthesized catalyst was denoted as HSZ(De-Al).

Chemical liquid deposition of tetra-ethoxysilane (CLD of TEOS): 1.0 g HSZ (H-type) and 25 ml n-hexane were added into a three-necked flask. It was stirred at 500 rpm under reflux. Then specific amount of TEOS (equal to 0.5 wt%, 1 wt% and 4 wt% SiO_2) was added. The reaction was kept for 1 h. Subsequently the n-hexane was removed by evaporation and the resultant materials was calcined at 550 ℃ for 4 h. The as-synthesized catalysts were denoted as HSZ(Si0.5), HSZ(Si1.0) and HSZ(Si4.0), respectively.

Characterization

The X-ray diffraction patterns (XRD) of synthesized materials were collected on a Rigaku D / Max 2200PC diffractometer equipped with Cu Kα radiation source (40 kV and 40 mA). The scanning rate and the angular step size were 5° min^{-1} and 0.02° respectively. The TEM images of synthesized materials were measured on a JEOL-2010F microscope at 200kV. SEM images were conducted on a FEI-Magellan 400L. Si/Al ratios of synthesized materials were determined by the Agilent Technologies 725 inductively coupled plasma optical emission spectrometry (ICP-OES). The ammonia temperature-programmed desorption (NH_3-TPD) profiles were measured on a Micromeritics Chemisorb 2750. N_2 absorption/desorption isotherms were conducted on Micromeritics ASAP 3000 porosity analyzer at 77K. The specific surface areas were calculated by the Brunauer–Emmett–Teller (BET) method and the pore size distributions were calculated by the Barrett–Joyner–Halenda (BJH) method. External surface areas and micropore volume were calculated by the *t*-plot method. The ^{27}Al NMR spectrums were recorded on a Bruker Avance III spectrometer. The gravimetric adsorption measurements were conducted with an intelligent gravimetric analyzer (IGA100, Hiden Analytical Ltd., Warrington, UK) at 25 ℃ using *m*-X and EB as sorbates.

Catalytic reactions

Isomerization of *o*-X: this catalytic reaction was conducted on a continuous flow microreactor equipping a quartz fixed-bed (i.d, 8 mm). 0.2 g catalyst particles (diameter of catalyst particles:

40~60 mesh) were pre-treated under 400 ℃ in N_2 flow (100 ml/min) for 2h. Then the microreactor was cooled down to 380 ℃. *o*-X was pumped into microreactor at the rate of 0.005 ml/min and the rate of N_2 flow was adjusted to 80 ml/min. The products were analyzed by an online gas chromatography of GC/2010 plus equipped with FID detector.

Catalytic cracking of 1,3,5-triisopropylbenzene (TIPB): This reaction was carried on a continuous flow microreactor. At first, 0.2 g catalysts with the diameter between 40 mesh to 60 mesh was activated at 500 ℃ under the N_2 flow (100 ml/min) for 2 h. Then TIPB was pumped into the microreactor at the rate of 0.002 ml/min and N_2 flow was switched to 30 ml/min. The products were analyzed by an online gas chromatography of GC/2010 plus equipped with a FID detector.

Competitive reaction of EB and *m*-X: The reaction was conducted on a continuous flow microreactor. At first, 0.2 g catalysts were activated at 500 ℃ under N_2 flow (100 ml/min) for 1 h. Then N_2 was switched to H_2 (the mole ratio of H_2:CH = 2) and the temperature was adjusted to 400 ℃. Subsequently, a mixture of EB and *m*-X (mole ratio = 1:4) was fed into the microreactor at the rate of WHSV = 6 h^{-1}. The products were analyzed by an online gas chromatography of GC/2010 plus equipped with FID detector.

Acknowledgements

This work was sponsored by the National Natural Science Foundation of China (21776297, U1510107, 21403303) and National Basic Research Program of China (2013CB933200).

Keywords: Hierarchically structured zeolites • surface passivation • shape-selectivity

[1] a) Y. Y. Fong, A. Z. Abdullah, A. L. Ahmad, S. Bhatia, *Chem. Eng. J.* **2008**, *139*, 172-193; b) A. Maneffa, P. Priecel, J. A. Lopez - Sanchez, *ChemSusChem*, **2016**, *9*, 2736-2748.

[2] a) J. H. Ahn, R. Kolvenbach, C. Neudeck, S. S. Al-Khattaf, A. Jentys, J. A. Lercher, *J. Catal.* **2014**, *311*, 271–280; b) P. Lu, Z. Y. Fei, L. Li, X. Z. Feng, W. J. Ji, W. P. Ding, Y. Chen, W. M. Yang, Z. K. Xie, *Appl. Catal. A- Gen.* **2013**, *453*, 302–309.

[3] Y. J. Ji, B. Zhang, L. Xu, H. H. Wu, H. G. Peng, L. Chen, Y. M. Liu, P. Wu, *J. Catal.* **2011**, *283*, 168–177.

[4] K. Miyake, Y. Hirota, K. Ono, Y. Uchida, S. Tanaka, N. Nishiyama, *J. Catal.* **2016**, *342*, 63–66.

[5] a) D. Verboekend, G. ViléH, J. Pérez-Ramírez, *Adv. Funct. Mater.* **2012**, *22*, 916–928. b) D. Verboekend, J. Pérez-Ramírez, *Catal. Sci. Technol.* **2011**, *1*, 879–890.

[6] a) K. Na, C. Jo, J. Kim, K. Cho, J. Jung, Y. Seo, R. J. Messinger, B. F. Chmelka, R. Ryoo, *Science*. **2011**, *333*, 328-332. b) X. Y. Zhang, D. X. Liu, D. D. Xu, S. Asahina, K. A. Cychosz, K, V. Agrawal, Y. A. Wahedi, A. Bhan, S. A. Hashimi, O. Terasaki, M. Thommes, M. Tsapatsis, *Science*. **2012**, *336*, 1684-1687.

[7] a) A. Ghorbanpour, A. Gumidyala, L. C. Grabow, S. P. Crossley, J. D. Rimer, *ACS nano.* **2015**, *9*, 4006-4016. b) S. Inagaki, K. Sato, S. Hayashi, J. Tatami, Y. Kubota, T. Wakihara, *ACS Appl. Mater. Interfaces*. **2015**, *7*, 4488-4493. c) G. Paparatto, E. Moretti, G. Leofanti, F. Gatti, *J. Catal.* **1987**, *105*, 227-232.

[8] a) H. B. Zhang, K. S. Song, L. Wang, H. X. Zhang, Y. H. Zhang, Y. Tang, *ChemCatChem.* **2013**, *5*, 2874-2878. b) C. Fernandez, I. Stan, J. P. Gilson, K. Thomas, A. Vicente, A. Bonilla, J. Pérez-Ramírez, *Chem. Eur. J.* **2010**, *16*, 6224 – 6233.

[9] a) J. H. Ahn, R. Kolvenbach, S. S. Al-Khattaf, A. Jentys, J. A. Lercher, *Chem. Commun.* **2013**, *49*, 10584–10586. b) J. G. Zhang, W. Z. Qian, C. Y. Kong, F. Wei, *ACS Catal.* **2015**, *5*, 2982-2988. c) N. Liu, X. X. Zhu, S. J. Hua, D. F. Guo, H. Y. Yue, B. Xue, Y. X. Li, *Catal. Commun*. **2016**, *77*, 60–64.

[10] a) D. Van Vu, M. Miyamoto, N. Nishiyama, Y. Egashira, K. Ueyama, *J. Catal.* **2006**, *243*, 389–394. b) Z. R. Zhu, Q. L. Chen, Z. K. Xie, W. M. Yang, D. J. Kong, C. Li, *J. Mol. Catal. A-Chem.* **2006**, *248*, 152-158.

[11] a) W. Tan, M. Liu, Y. Zhao, K. K. Hou, H. Y. Wu, A. F. Zhang, H. O. Liu, Y. R. Wang, C, S. Song, X. W. Guo, *Micropor. Mesopor. Mater*. **2014**, *196*, 18–30. b) Y. T. Cheng, Z. P. Wang, C. J. Gilbert, W. Fan, G. W. Huber, *Chem. Int. Ed.* **2012**, *51*, 11097–11100. c) S. R. Zheng, H. R. Heydenrych, A. Jentys, J. A. Lercher, *J. Phys. Chem. B.* **2002**, *106*, 9552-9558. d) S. R. Zheng, H. R. Heydenrych, H.P. Röger, A. Jentys, J. A. Lercher, *Top. Catal.* **2003**, *22*, 101-106. e) A. Vogt, H. W. Kouwenhoven, R. Prins, *Appl. Catal. A- Gen.* **1995**, *123*, 37-49.

[12] a) T. G. Ge, Z. L. Hua, X. Y. He, J. Lv, H. R. Chen, L. X. Zhang, H. L. Yao, Z. W. Liu, C. C. Lin, J. L. Shi, *Chem. Eur. J.* **2016**, *22*, 7895-7905. b) R. Giudici, H. W. Kouwenhoven, R. Prins, *Appl. Catal. A- Gen.* **2000**, *203,* 101-110.

[13] H. L. Hu, J. H. Lyu, J. Y. Rui, J. Cen, Q. F. Zhang, Q. T. Wang, W. W. Han, X. N. Li, *Catal. Sci. Technol.* **2016**, *6*, 2647-2652.

[14] X. Y. He, T. G. Ge, Z. L. Hua, J. Zhou, J. Lv, J. L. Zhou, Z. C. Liu, J. L. Shi, *ACS Appl. Mater. Interfaces.* **2016**, *8*, 7118-7124.

[15] a) Y. S. Bhat, J. Das, A. B. Halgeri, *Appl. Catal. A-Gen.* **1994**, *115*, 257-267; b) S. Y. Zheng, A. Jentys, J. A. Lercher, *J. Catal.* **2006**, *241*, 304-311; c) V. J. Frilette, W. O. Haag, R. M. Lago, *J. Catal.* **1981**, *67*, 218–222; d) T. Biligetu, Y. Wang, T. Nishitoba, R. Otomo, S. Park, H. Mochizuki, J. N. Kondo, T. Tatsumi, T. Yokoi, *J. Catal.* **2017**, 353, 1-10. e) T. Yokoi, H. Mochizuki, T. Biligetu, Y. Wang, T. Tatsumi, *Chem. Lett.* **2017**, *4*, 798-800. f) J. Jae, G. A. Tompsett, A. J. Foster, K. D. Hammond, S. M. Auerbach, R. F. Lobo, G. W. Huber, *J. Catal.* **2011**, *279*, 257-268.

[16] a) Y. G. Li, H. Jun, *Appl. Catal. A-Gen.* **1996**, *142*, 123-137; b) J. L. Hodala, Y. S. Bhat, A. B. Halgeri, G. V. Shanbhag, *Chem. Eng. Sci.* **2015**, *138*, 396-402.

[17] a) X. Hou, Y. Qiu, E. X. Yuan, X. W. Zhang, G. Z. Liu, *Appl. Catal. A-Gen.* **2017**, *537*, 12-23; b) S. J. Reitmeier, O. C. Gobin, A. Jentys, J. A. Lercher, *Angew. Chem. Int. Ed.* **2009**, *48*, 533 –538. c) J. J. Zheng, Q. H. Zeng, Y. Y. Zhang, Y. Wang, J. H. Ma, X. W. Zhang, W. F. Sun, R. F. Li, *Chem. Mater.* **2010**, *22,* 6065–6074.

[18] a) Y. Seo, K. Cho, Y. Jung, R. Ryoo, *ACS Catal*. **2013**, *3*, 713-720; b) I. Kahle, S. Spange, *J. Phys. Chem. C.* **2010**, *114*, 15448–15453; c) Q. Zhao, W. H. Chen, S. J. Huang, Y. C. Wu, H. K. Lee, S. B. Liu, *J. Phys. Chem. B.* **2002**, *106*, 4462-4469.

10.1002/cctc.201800044

Entry for the Table of Contents

FULL PAPER

1. Hierarchically structured ZSM-5 zeolites (HSZ) were synthesized and passivated by dealumination or CLD of TEOS.

2.Surface-passivated HSZ showed remarkably enhanced shape-selectivity (*p*-X selectivity) and improved catalytic activity than the microporous ZSM-5 counterparts in the model reaction of *o*-X isomerization.

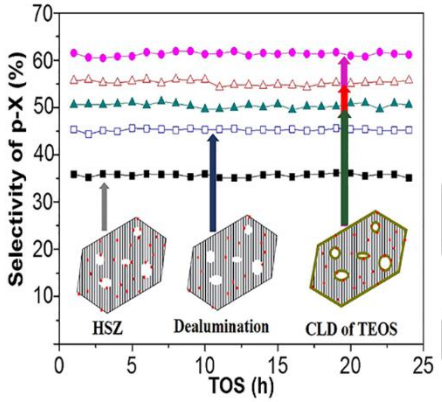

Jian Lv, Zile Hua, Jian Zhou, Zhicheng Liu, Hangle Guo and Jianlin Shi. **

Page No. – Page No.

Surface-passivated hierarchically structured ZSM-5 zeolites: high-performance shape-selective catalysts for *para*-xylene production